Oleaginous Microalga *Coccomyxa subellipsoidea* as a Highly Effective Cell Factory for CO_2 Fixation and High-Protein Biomass Production by Optimal Supply of Inorganic Carbon and Nitrogen

Yu Liu[1], Dong Wei[1,2]* and Weining Chen[3]

[1]School of Food Science and Engineering, Guangdong Province Key Laboratory for Green Processing of Natural Products and Product Safety, Engineering Research Center of Starch and Vegetable Protein Processing Ministry of Education, South China University of Technology, Guangzhou, China, [2]Research Institute for Food Nutrition and Human Health, Guangzhou, China, [3]School of Chemical and Biomedical Engineering, Nanyang Technological University, Singapore, Singapore

Microalgae used for CO_2 biofixation can effectively relieve CO_2 emissions and produce high-value biomass to achieve "waste-to-treasure" bioconversion. However, the low CO_2 fixation efficiency and the restricted application of biomass are currently bottlenecks, limiting the economic viability of CO_2 biofixation by microalgae. To achieve high-efficient CO_2 fixation and high-protein biomass production, the oleaginous microalga *Coccomyxa subellipsoidea* (*C. subellipsoidea*) was cultivated autotrophically through optimizing inorganic carbon and nitrogen supply. $0.42 \, g \, L^{-1}$ $NaHCO_3$ supplemented with 2% CO_2 as a hybrid carbon source resulted in high biomass concentration ($3.89 \, g \, L^{-1}$) and productivity (318.33) with CO_2 fixation rate $544.21 \, mg \, L^{-1} \, d^{-1}$ in shake flasks. Then, used in a 5-L photo-fermenter, the maximal protein content (60.93% DW) in batch 1, and the highest CO_2 fixation rate ($1043.95 \, mg \, L^{-1} \, d^{-1}$) with protein content (58.48% DW) in batch 2 of repeated fed-batch cultures were achieved under $2.5 \, g \, L^{-1}$ nitrate. The relative expression of key genes involved in photosynthesis, glycolysis, and protein synthesis showed significant upregulation. This study developed a promising approach for enhancing carbon allocation to protein synthesis in oleaginous microalga, facilitating the bioconversion of the fixed carbon into algal protein instead of oil in green manufacturing.

Keywords: oleaginous microalga, *Coccomyxa subellipsoidea*, CO_2 fixation, high-protein biomass, photo-fermenter

---

Abbreviations: CCU, carbon capture and utilization; NR, nitrate reductase; NIR, nitrite reductase; GS/GOGAT, glutamine synthetase/glutamine oxoglutarate aminotransferase or glutamate synthase cycle; DIC, dissolved inorganic carbon; DW, biomass dry weight; R_{CO_2}, CO_2 fixation rate; and DLU, degree of lipid unsaturation.

1 INTRODUCTION

Global climate change results from a massive emission of greenhouse gases (Blunden and Arndt, 2020; Pielke et al., 2022). Nowadays, CO$_2$ concentration in the atmosphere has exceeded 400 ppm, mainly caused by the combustion of fossil fuels. CO$_2$ biofixation by microalgae has obvious advantages on higher photosynthetic efficiency, faster cell growth, better environmental adaptability, and more high-value biomass coproduction than the higher plant and, thus, has been regarded as a promising approach for carbon capture and utilization (CCU) (Zhou et al., 2017; Cheng et al., 2019). However, the biotic (mainly biocontamination) and abiotic (water, weather, and material supply) factors leading to low algal biomass production are the bottlenecks restricting its application in the current agriculture-mode cultivation system of microalgae (Ruiz et al., 2016). Hence, enhancing the CO$_2$ biofixation capacity of microalgae remains an urgent topic for sustainable biomass production and further value-added utilization.

Inorganic carbon source is the most critical factor for cell growth and CO$_2$ fixation by autotrophic microalgae. Usually, dissolved CO$_2$ and HCO$_3^-$ can be utilized as carbon sources, but low CO$_2$ solubility limits the use for algal growth (Song et al., 2019b). To overcome this obstacle, bicarbonate can serve as a chemical absorbent to accelerate CO$_2$ dissolution in an alkalic environment and is also a carbon source for microalgal growth (Song et al., 2019a), integrating the chemical absorption of CO$_2$ with biofixation effectively. For example, the addition of 50 mM bicarbonate with 5% CO$_2$ achieved a 27% increase in biomass productivity by *C. vulgaris* (Lohman et al., 2015). Hybrid CO$_2$ capture based on bicarbonate to culture *Chlorella* sp. achieved a carbon conversion efficiency of over 60% (Song et al., 2019c). A 42% increase in cell growth of *Chlorella* sp. was achieved by supplying 5.0 g L^{-1} NaHCO$_3$ to absorb CO$_2$ (Tu et al., 2018). Hence, chemical absorption of CO$_2$ coupled with biofixation as a hybrid CCU strategy is a promising approach for CO$_2$ fixation and biomass production by microalgae.

Inorganic carbon assimilated *via* microalgae is further converted into various biochemical components including proteins, carbohydrates, lipids, and pigments. Recently, microalgae have been regarded as a novel protein source for meat analogs, which not only provides more nutritional ingredients compared to conventional plant-based protein but also reduces greenhouse gas emissions by replacing part of livestock breeding and farming (Fu et al., 2021). In addition to carbon sources, nitrogen is another core factor for microalgal growth, as a key element in amino acids, protein, and enzymes (Yadav et al., 2021). The nitrogen level in the medium directly affects nitrogen uptake (Wu and Miao, 2014) and the transcription of genes involved in nitrogen assimilation (Miller et al., 2010). A high level of nitrate can induce the high expression of genes related to nitrogen assimilation, such as nitrate reductase (NR) and nitrite reductase (NIR) (Chen et al., 2012). Abundant nitrate is transported into the cells and reduced to ammonium and further incorporated into α-oxoglutarate in the TCA cycle through the glutamine synthetase/glutamine oxoglutarate

aminotransferase or glutamate synthase (GS/GOGAT) cycle for protein synthesis (Su, 2021). Additionally, replete nitrogen in the medium leads to nitrogen-rich algae cells with an intracellular C/N ratio of 6~7 (Huang et al., 2018); thus, it is unnecessary to degrade the intra-nitrogen pool, including proteins, amino acids, and chlorophylls, for maintaining the cell growth. Conversely, the deprived nitrogen can result in an unbalanced intra-C/N ratio, and then the main nitrogen compounds are degraded to respond to the emergent demand for nitrogen. The previous study reported that the protein content of *Scenedesmus* sp. dramatically decreased by 70% (Pancha et al., 2014) and a 15% decline in *Chlamydomonas reinhardtii* (Dean et al., 2010) under nitrogen limitation, but the lipid content in these algae increased inversely. It suggested that maintaining a relatively high level of nitrogen in the medium can promote the photosynthetic carbon flow into protein synthesis by enhanced nitrogen assimilation.

As the first sequenced species of eukaryotic microalgae from the polar region, *C. subellipsoidea* is realized as an oleaginous microalga for biofuel production with the relatively fragile cell wall and many more genes involved in lipid biosynthesis (Blanc et al., 2012). Currently, most of the studies concerned the performance of *C. subellipsoidea* for lipid accumulation under nitrogen depletion, such as, high lipid content of 50.5% DW (Wang et al., 2017) and 52.16% DW under nitrogen limitation (Wang et al., 2019). Whereas lipid accumulation is generally achieved at the expense of cell growth under nitrogen deprivation (Corteggiani Carpinelli et al., 2014); additionally, *C. subellipsoidea* was only applied to biodiesel production, restricting its application potential in multiple areas, which further reduced the economic viability of *C. subellipsoidea* cultivation. In our previous study, a 2% CO$_2$ supply could improve biomass productivity by encouraging autotrophic growth of *C. subellipsoidea* (Peng et al., 2016), suggesting the technical feasibility for CO$_2$ fixation using *C. subellipsoidea*. However, so far, little is known about the potential application of this oleaginous microalga for enhancing CO$_2$ fixation and protein coproduction by autotrophy simultaneously.

This study aimed to develop a hybrid CCU strategy for high-efficient CO$_2$ fixation and high-protein biomass production through a combination of chemical absorption of CO$_2$ and biofixation by autotrophic *C. subellipsoidea*. The hybrid carbon source optimized in shake flasks was further used in the batch and repeated fed-batch cultures with the optimized nitrogen supply in 5-L photo-fermenters. The expression of key genes involved in the central carbon and nitrogen metabolism was analyzed to reveal the regulation of enhanced CO$_2$ fixation and carbon allocation to proteins synthesis in the cells.

2 MATERIALS AND METHODS

2.1 Microalgae Strain and Seed Culture

The oleaginous microalga *C. subellipsoidea* was purchased from the Microbial Culture Collection of the National Institute for Environmental Studies (NIES) in Japan, with strain number NIES 2166. The seed culture was performed in 250-ml Erlenmeyer

flasks containing 100 ml basal medium (Wang et al., 2019) with a modified concentration of $NaNO_3$ (1.25 g L^{-1}) and glucose (2.00 g L^{-1}) as carbon source. The temperature was set at 25°C under continuous white LED of 80 µmol m^{-2} s^{-1} in a shaking incubator at 160 rpm.

2.2 Optimization of Inorganic Carbon Source in Shake Flasks

To explore the optimal inorganic carbon source for CO_2 fixation, the autotrophic growth of *C. subellipsoidea* was conducted under the following conditions: 0.42 g L^{-1} $NaHCO_3$ was added to the basal medium as the control. 2% CO_2; 0.42, 0.63, and 0.84 g L^{-1} $NaHCO_3$ with 2% CO_2 supplementation were set up as the testing carbon source with 1.25 g L^{-1} $NaNO_3$. The seed was inoculated into the 100 ml basal medium in 250-ml shake flasks with an initial cell density of about 1×10^7 ml^{-1}, and the other conditions were the same as the seed culture. The sample was taken every 2 days for measuring cell density, biomass concentration, and pH value. The nutrient composition, intracellular carbon and nitrogen contents in biomass, and dissolved inorganic carbon (DIC) in the medium were detected at the end of the cultures.

2.3 Batch and Repeated Fed-Batch Cultures in 5-L Photo-Fermenters

To verify the effect of the optimal carbon source obtained earlier, the batch culture was implemented in a 5-L photo-fermenter with automatic control of pH and temperature (25°C). The stock solution containing 8.4 g L^{-1} $NaHCO_3$ was filtrated through a 0.22 µm membrane for removing bacteria and then added into the basal medium for a final concentration of 0.42 g L^{-1}. Then, 2% CO_2 was sparged continuously into the photo-fermenter controlled by a gas mass flow meter. The initial pH value was around 7.0 and then maintained at 8.0 by adding 0.5 M HCl solution during the incubation period. Four white LED panels were installed surrounding the glass fermenter to supply adjustable light intensity from 80 to 200 µmol m^{-2} s^{-1}. The stirring speed was set from 150 to 300 rpm, and the aeration rate (1:1, *vvm*) was set at 4 L min^{-1} by pressed air. A gradient adjustment of light intensity and the stirring speed was set up with the increasing cell density. Especially, the initial $NaNO_3$ concentration was increased to 2.5 g L^{-1} in the photo-fermenter to avoid fast depletion of nitrogen like 1.25 g L^{-1} $NaNO_3$ in shake flasks.

To further enhance CO_2 fixation, the repeated fed-batch cultures were carried out subsequently to relieve light limitation resulting from the deep green color caused by the high cell density in the batch culture. Batch 1 was performed in the basal medium containing 0.42 g L^{-1} $NaHCO_3$ with 2% CO_2 and 2.5 g L^{-1} $NaNO_3$ for 6 days, and then 3 L culture liquor was pumped out and replaced by the same volume of the previous fresh basal medium, starting the batch 2 culture for another 7-days culture. The other culture conditions were the same as for the batch culture. The sample was taken to detect cell density every 24 h, and chlorophylls, intracellular carbon and nitrogen contents in biomass, and nitrate concentration in the medium

were detected each 48 h. The nutrient composition in biomass was detected at the beginning and end of cultures.

2.4 Key Gene Expression Analysis for the Culture in 5-L Photo-Fermenters

To reveal the regulation of central carbon and nitrogen metabolism during autotrophic growth in 5-L photo-fermenters, the samples were taken at 192 h in the batch culture and at 48, 120, 144, 192, and 288 h in repeated fed-batch cultures for analysis of key genes' expression levels, and then, the regulatory pathways were proposed.

2.5 Analytical Methods
2.5.1 Cell Growth
Cell density was detected by CytoFLEX flow cytometry (Beckman-Coulter, United States); biomass dry weight (DW) was determined by the gravimetric method (Zhu et al., 2022); and specific growth rate, µ (d^{-1}), was calculated according to the formula (Zhu et al., 2022).

2.5.2 NO_3^- Uptake and CO_2 Fixation Rate
NO_3^- concentration was determined using a multi-parameter water analyzer (HANNA, Italy) with the appropriative reagent. A total carbon analyzer (Vario TC, Elementar, Germany) was used to detect DIC in the medium. The intracellular carbon (Cc, % w/w) and nitrogen content (Nc, % w/w) were assayed using an element analyzer (Elementar, Germany), and then CO_2 fixation rate (R_{CO2}) and intracellular C/N ratio were calculated as follows:

$$R_{CO_2}\left(mg\,L^{-1}d^{-1}\right) = C_C P \frac{M_{CO_2}}{M_C}, \qquad (1)$$

$$Intra - C/N\ ratio = \frac{Cc/M_C}{Nc/M_N}, \qquad (2)$$

where P is the biomass productivity (mg L^{-1} d^{-1}), M_C and M_N are the molecular weight of carbon and nitrogen, respectively, and M_{CO2} is the molecular weight of CO_2.

2.5.3 Nutrient Composition in Biomass
Protein content was determined by the Kjeldahl method (Chen and Vaidyanathan, 2013). Amino acid content and profile were analyzed according to the methods (Zhu et al., 2022) with modification. Briefly, 100 mg of lyophilized biomass powder was hydrolyzed with 5 ml of hydrochloric acid (6 mol L^{-1}) in a water bath at 110°C for 24 h. The hydrolyzed sample was cooled to room temperature and filtered with a funnel and diluted to 25 ml. After that, 2 ml of the above sample was deacidified and then followed by the addition of 1 ml of 0.02 mol L^{-1} HCl as a buffer solution. Finally, 20 µl of the filtered sample was detected by an amino acid analyzer. Carbohydrate content was determined using the phenol-sulfuric acid method (Chen and Vaidyanathan, 2013). Total lipid content, fatty acids content, and profile were analyzed according to the previous study (Chen and Wei, 2015; Chen et al., 2021). Pigments were extracted by acetone (90%, v/v), and the qualitative and quantitative
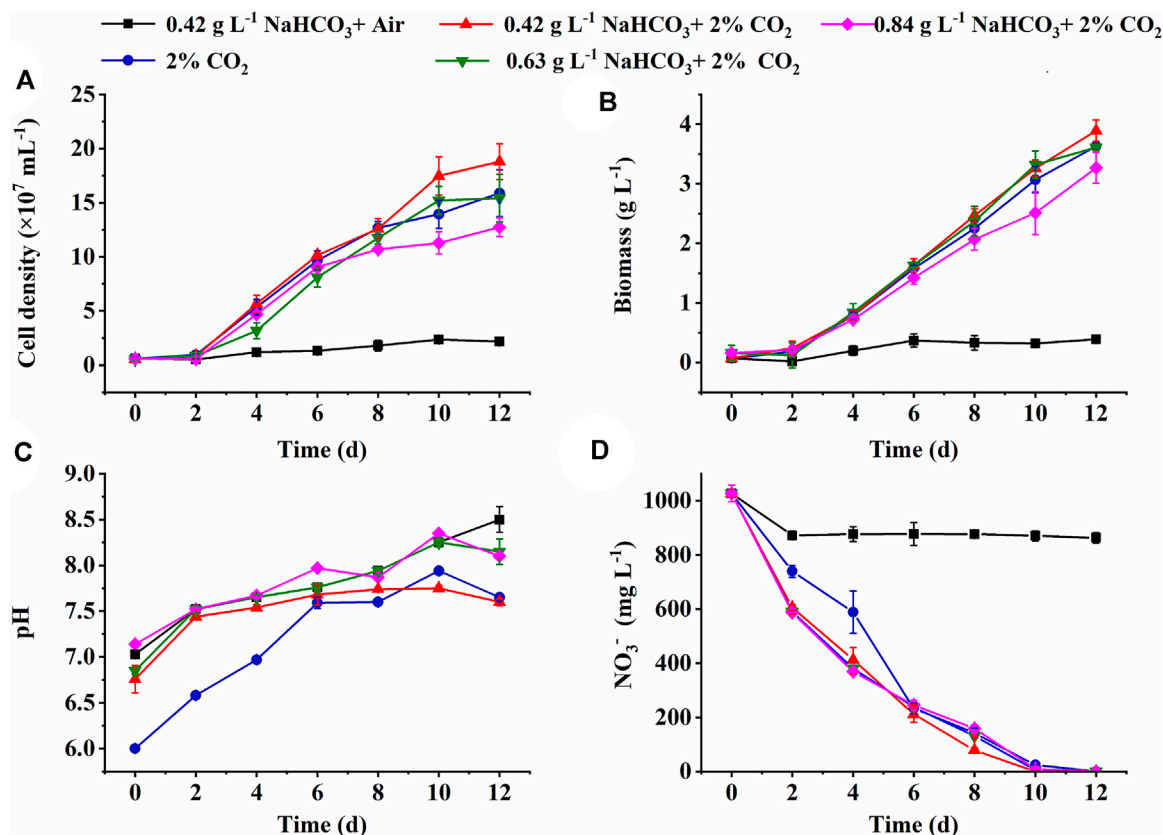
FIGURE 1 | Effect of inorganic carbon source on the cell growth **(A)**, biomass production **(B)**, pH changes **(C)**, and NO_3^- consumption **(D)** in the medium by autotrophic *C. subellipsoidea* in shake flasks.

analysis of chlorophyll and carotenoids were carried out using the described method (Wang et al., 2020).

2.5.4 Assay of Key Gene Expression Levels by qRT-PCR

Total RNA was extracted from fresh cells using TRIZOL (Invitrogen, Carlsbad, United States). RNA quality and quantity were evaluated by a micro-spectrophotometer (LabTech, Holliston, United States) (**Supplementary Table S1**). Evo M-MLV kit (Accurate Biotechnology, China) was employed to obtain cDNA, and qRT-PCR was performed on a real-time PCR detection system (Bio-rad, United States). The gene coding ribosomal protein L5 (*RibL5*) was used as the internal control (Peng et al., 2016). The primers (**Supplementary Table S2**) were designed by NCBI (https://www.ncbi.nlm.nih.gov/tools/primer-blast/), and the sequence of target genes was also searched in NCBI. The relative expression levels of target genes were normalized using *RibL5* as a reference gene by the $2^{-\Delta\Delta Ct}$ method (Peng et al., 2016).

2.6 Statistical Analysis

All data are presented as the means ± standard deviation (SD) from three replicates. Statistical analyses were carried out using Origin 9.0 software. The statistical significance was evaluated using a one-way analysis of variance (ANOVA) and LDS *t*-test with SPSS 26.0, and then, the significant levels were set at $p < 0.05$.

3 RESULTS AND DISCUSSION

3.1 Effects of Inorganic Carbon Source on Cell Growth and CO_2 Fixation in Shake Flasks

The cell growth under various inorganic carbon sources is shown in **Figure 1**. The constant increase of cell density and biomass concentration was observed in all cultures supplemented with 2% CO_2, much higher than the control (0.42 g L^{-1} NaHCO$_3$ with air) (**Figures 1A,B**). The highest biomass yield (3.82 g L^{-1}) and productivity (318.33 mg L^{-1} d^{-1}) with final cell density (1.88 × 10^8 ml^{-1}) and R_{CO2} (544.21 mg L^{-1} d^{-1}) were achieved under 0.42 g L^{-1} NaHCO$_3$ with 2% CO_2 (**Table 1**), 11.94-fold, 11.94-fold, 31.6-fold, and 13.3-fold higher than the control ($p < 0.05$), respectively. These results indicated that 0.42 g L^{-1} NaHCO$_3$ with 2% CO_2 was the optimal carbon source for biomass production and CO_2 fixation, which was consistent with the previous reports that the highest biomass productivity (0.14 g L^{-1} d^{-1}) of *C. vulgaris* was achieved under 5 mmol L^{-1} NaHCO$_3$ with 5%

TABLE 1 | Biomass production, CO$_2$ photosynthetic fixation, and nitrate uptake by autotrophic *C. subellipsoidea* under various inorganic carbon sources in shake flasks.

Variable	Inorganic carbon source				
	0.42 g L^{-1} NaHCO$_3$ + air	2% CO$_2$	0.42 g L^{-1} NaHCO$_3$ + 2% CO$_2$	0.63 g L^{-1} NaHCO$_3$ + 2% CO$_2$	0.84 g L^{-1} NaHCO$_3$ + 2% CO$_2$
Biomass production					
Yield (g L^{-1})	0.32 ± 0.06[e]	3.43 ± 0.26[c]	3.82 ± 0.18[ab]	3.61 ± 0.26[bc]	3.11 ± 0.2[d]
Productivity (mg L^{-1} d^{-1})	26.67 ± 0.50[e]	285.83 ± 5.67[c]	318.33 ± 1.52[ab]	300.83 ± 2.16[bc]	259.17 ± 16.67[d]
CO2 fixation					
Intracellular carbon (% DW)	45.64 ± 0.56[b]	48.58 ± 0.03[a]	48.77 ± 0.15[a]	48.60 ± 0.21[a]	48.61 ± 0.04[a]
Extracellular DIC (mg L^{-1})	9.69 ± 0.57[e]	41.40 ± 1.90[d]	51.00 ± 1.93[c]	58.58 ± 0.88[b]	79.16 ± 0.37[a]
R$_{CO2}$ (mg L^{-1} d^{-1})	40.91 ± 0.50[e]	523.10 ± 0.55[b]	544.21 ± 0.17[a]	515.51 ± 0.30[c]	443.67 ± 1.70[d]
Nitrate uptake					
NO$_3^-$ uptake rate (mg L^{-1} d^{-1})	13.63 ± 2.03[c]	100.25 ± 2.56[b]	118.50 ± 1.59[a]	102.18 ± 3.15[b]	101.75 ± 2.50[b]
Intracellular nitrogen (% DW)	6.21 ± 0.33[b]	5.51 ± 0.26[b]	5.34 ± 0.11[c]	6.57 ± 0.09[a]	6.12 ± 0.03[b]
Intracellular C/N ratio	7.78 ± 0.01[d]	10.31 ± 0.50[b]	10.66 ± 0.50[a]	9.14 ± 0.12[c]	9.27 ± 0.19[c]

Different letters in superscripts within one row present a significant difference (p < 0.05). Letters denoted the differentiation among different inorganic carbon sources.

CO$_2$ as the carbon source (Lohman et al., 2015). More encouragingly, compared to the latest reports so far, R$_{CO2}$ (544.21 mg L^{-1} d^{-1}) obtained in the shake flasks was superior to that of 360.12 mg L^{-1} d^{-1} for *Chlorella fusca* (Zhu et al., 2020), 350.0 mg L^{-1} d^{-1} for *Scenedesmus* sp. (Rodas-Zuluaga et al., 2021), 470.0 mg L^{-1} d^{-1} for *Chlorella* sp. (Yadav et al., 2020), and 350.0 mg L^{-1} d^{-1} for *N. oceanica* (Wang et al., 2022) by autotrophic culture in shake flasks. These results might be attributed to the sufficient DIC supplied by CO$_2$ and NaHCO$_3$ as the hybrid carbon sources in the medium for photosynthesis. It was observed that the DIC concentration (51~79 mg L^{-1}) under hybrid carbon sources was significantly higher than that of around 10 mg L^{-1} under 0.42 g L^{-1} NaHCO$_3$ and 41 mg L^{-1} under 2% CO$_2$, respectively, but the excess DIC under 0.63 and 0.84 g L^{-1} NaHCO$_3$ with 2% CO$_2$ supplement was shown to decrease the biomass yield and R$_{CO2}$ (**Table 1**).

In addition to DIC, the most stable pH in the medium was also observed under the optimal carbon source (0.42 g L^{-1} NaHCO$_3$ and 2% CO$_2$) with the minimum pH fluctuation at 1.15, compared to 1.47 in the control and around 1.94 in the other two cultures (**Figure 1C**). It was reported that bubbled CO$_2$ captured by the hybrid carbon source (NaHCO$_3$ and CO$_2$) and stored as HCO$_3^-$ could drop the pH value in the medium and weaken the effect of pH rise resulting in nitrate and HCO$_3^-$ consumption *via* algal cell growth (Wang et al., 2018; Zhu et al., 2020). When HCO$_3^-$ is utilized, OH$^-$ can be released and then recycled to capture subsequent CO$_2$ to form bicarbonate again (Gardner et al., 2012). The advantage of the optimal carbon source provided an effective buffer system for steady pH and sufficient DIC for photosynthesis.

It is also noticed that nitrate almost ran out on the 8th day in the group of hybrid carbon sources (**Figure 1D**), where NO$_3^-$ uptake rate was significantly higher than that of the single carbon sources (0.42 g L^{-1} NaHCO$_3$ or 2% CO$_2$). The highest NO$_3^-$ uptake rate (118.50 mg L^{-1} d^{-1}) under the optimal carbon source was 8.7-fold higher than that of the control (13.63 mg L^{-1} d^{-1}) (**Table 1**) due to the rapid cell growth. It resulted in the N-depletion, and then the low nitrogen with high carbon content intracellularly led to the unbalanced C/N ratio of 9 ~

11, which exceeded the normal range of 6–7 in algae cells (Huang et al., 2018), under hybrid carbon sources or 2% CO$_2$ (**Table 1**); thus, the slow increase of cell density and biomass accumulation from the 8th day to the end of culture might be caused by the N-depletion (**Figures 1A,B**). The results suggested that sufficient nitrogen is critical to maintain the balanced C/N ratio intracellularly for fast cell growth and CO$_2$ fixation. Thus, the nitrate concentrate should be elevated in the following experiments.

3.2 Cell Growth and CO$_2$ Fixation in the Batch and Repeated Fed-Batch Cultures in 5-L Photo-Fermenters

To verify the effect of the optimal hybrid carbon source and optimize nitrate concentrations in a scale-up culture, the batch and repeated fed-batch cultures were conducted in 5-L photo-fermenters. In **Figure 2A**, a slow increase of biomass concentration within the first 48 h in the batch culture was observed, and then it increased constantly till the stationary phase, along with biomass yield (1.75 g L^{-1}) and productivity (175.00 mg L^{-1} d^{-1}) (**Table 2**). The long stationary phase lasted from 192 h to the end of the culture; this might be due to the limitation of effective depth of light penetration (Pilon et al., 2011), resulting in dark green color by increasing cell density. Although the gradient adjustment of light intensity and stirring speed could improve the mixing and reduce the light-shading effect to some extent, the algal cells still lack adequate light required by photosynthesis. It implies that the well-distributed light field inside a photobioreactor is still the key challenge for the larger-scale cultivation of microalgae (Sun et al., 2016). The intracellular chlorophylls, carbon content, and R$_{CO2}$ increased at the exponential phase and then decreased synchronously, and the average R$_{CO2}$ (252.18 mg L^{-1} d^{-1}) was obtained along with the intracellular carbon (39.3% DW) and chlorophylls content (12.9 mg g^{-1}). It was noticed that the content of intracellular substances, like chlorophylls, carbon, and nitrogen showed a strong fluctuation in the first 48 h (**Figure 2A**). It might be ascribed that microalgal cells required new homeostasis
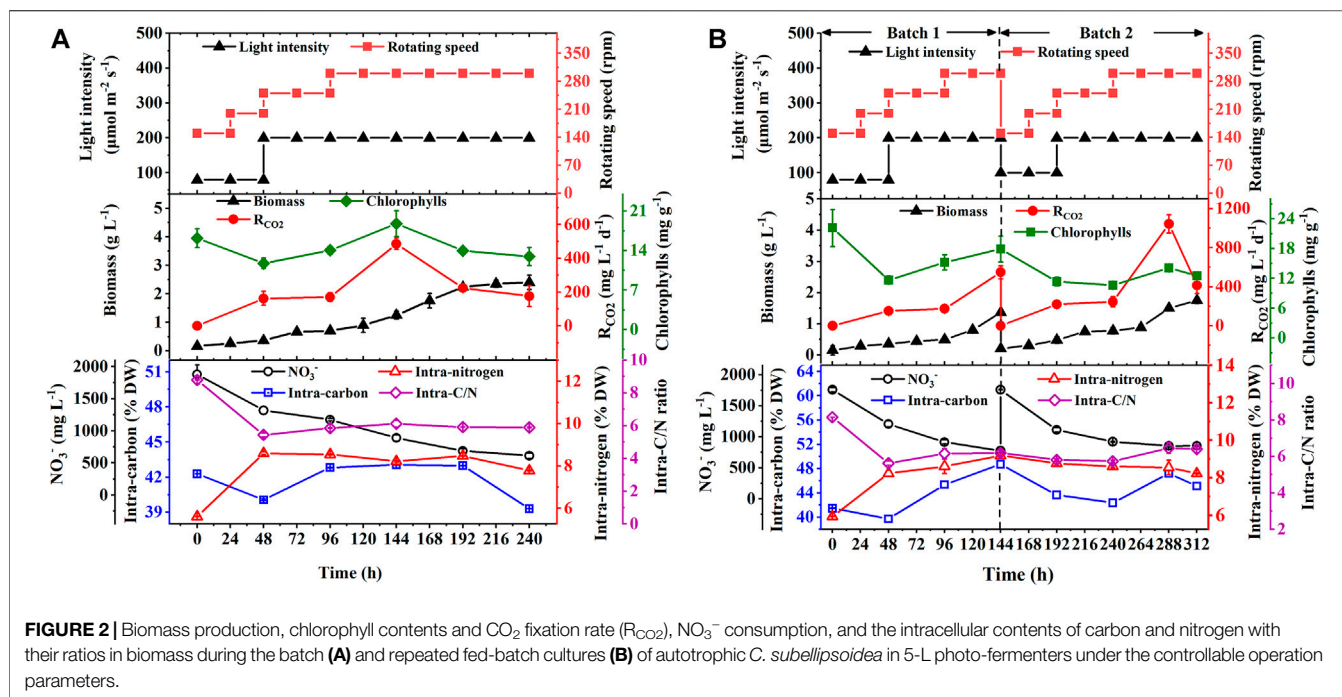
FIGURE 2 | Biomass production, chlorophyll contents and CO_2 fixation rate (R_{CO2}), NO_3^- consumption, and the intracellular contents of carbon and nitrogen with their ratios in biomass during the batch **(A)** and repeated fed-batch cultures **(B)** of autotrophic *C. subellipsoidea* in 5-L photo-fermenters under the controllable operation parameters.

TABLE 2 | Biomass production, CO_2 fixation, and nitrate uptake by autotrophic *C. subellipsoidea* during the batch and repeated fed-batch cultures under 2.5 g L^{-1} $NaNO_3$ in 5-L photo-fermenters.
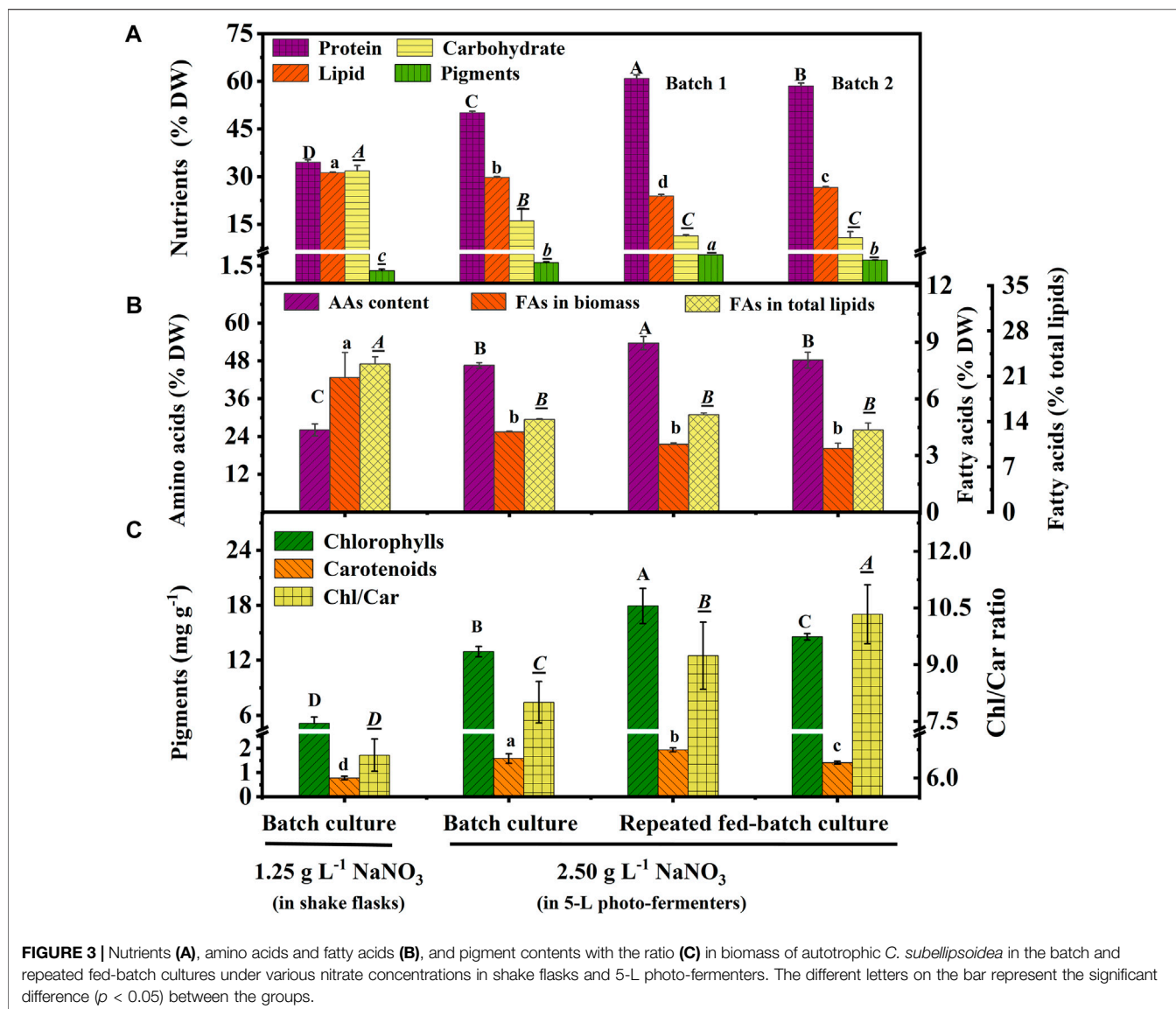
Variable	Batch culture	Repeated fed-batch culture	
		Batch 1	Batch 2
Biomass production			
μ (d^{-1})	0.25 ± 0.02[b]	0.30 ± 0.01[b]	0.37 ± 0.02[a]
Yield (g L^{-1})	1.75 ± 0.11	1.23 ± 0.04	1.54 ± 0.01
Productivity (mg L^{-1} d^{-1})	175.00 ± 9.00[c]	204.17 ± 5.67[b]	220.28 ± 1.43[a]
CO2 fixation and nitrate uptake rate			
Ave. R_{CO2} (mg L^{-1} d^{-1})	252.18 ± 3.54[b]	364.57 ± 1.68[a]	364.43 ± 0.57[a]
Max. R_{CO2} (mg L^{-1} d^{-1})	484.93 ± 4.98[c]	848.19 ± 25.67[b]	1043.95 ± 72.01[a]
NO_3^- uptake rate (mg L^{-1} d^{-1})	126.56 ± 6.82[b]	168.75 ± 10.83[a]	128.78 ± 4.85[b]
Final concentration of NO_3^- (mg L^{-1})	610.90 ± 39.88[b]	774.75 ± 18.03[a]	855.00 ± 12.73[a]

The significant difference of p < 0.05 is presented between the batch and repeated fed-batch cultures.

established *via* metabolic regulation when it was transferred from the shake flask to the photo-fermenter or fresh medium was added into the culture (Moejes et al., 2017). Regarding nitrogen assimilation, it was found that NO_3^- concentration constantly decreased with uptake rate (126.56 mg L^{-1} d^{-1}) and remained at 610.90 mg L^{-1} at the end of culture under 2.5 g L^{-1} $NaNO_3$ (**Table 2**). The intracellular nitrogen content and C/N ratio were kept stable at around 8% DW and six, respectively, from 48 h to the end of the culture (**Figure 2A**). The sufficient nitrate in the medium and balanced intracellular C/N ratio suggested that the slow increase of biomass concentration and the decline of R_{CO2} after 144 h were caused by the light attenuation instead of the decreased nitrogen.

To overcome the drawback, repeated fed-batch culture was adopted to weaken light attenuation by renewing the culture liquor through harvesting biomass and replacing fresh medium.

The biomass concentration and R_{CO2} constantly increased to 1.37 g L^{-1} and 548.19 mg L^{-1} d^{-1} in batch 1, respectively, and then an exponential phase of cell growth was observed again in batch 2 (**Figure 2B**). As summarized in **Table 2**, the specific growth rate (0.30 d^{-1} and 0.37 d^{-1}), biomass productivity (204.17 mg L^{-1} d^{-1} and 220.28 mg L^{-1} d^{-1}), and average R_{CO2} (364.57 mg L^{-1} d^{-1} and 364.43 mg L^{-1} d^{-1}) in batch 1 and batch 2 of repeated fed-batch culture were significantly 1.2-~1.5-fold, 1.2-~1.3-fold, and 1.5-fold higher than those of the batch culture in 5-L photo-fermenters, respectively ($p < 0.05$). Especially, the maximum R_{CO2} (1043.95 mg L^{-1} d^{-1}) in batch 2 was 2.2-fold higher than that of 484.93 mg L^{-1} d^{-1} in the batch culture ($p < 0.05$). The enhanced biomass production and CO_2 fixation in repeated fed-batch culture indicated that biomass harvesting and medium renewing could effectively relieve lighting shade. The previous study also reported that

FIGURE 3 | Nutrients **(A)**, amino acids and fatty acids **(B)**, and pigment contents with the ratio **(C)** in biomass of autotrophic *C. subellipsoidea* in the batch and repeated fed-batch cultures under various nitrate concentrations in shake flasks and 5-L photo-fermenters. The different letters on the bar represent the significant difference ($p < 0.05$) between the groups.

maintaining suitable cell density through biomass harvesting could provide abundant light for photophosphorylation, which further produced more assimilatory power (ATP and NADPH) for CO$_2$ fixation (Naduthodi et al., 2021). Additionally, R$_{CO2}$, intracellular chlorophylls, and carbon content in the two batch cultures also exhibited synchronized change trends in the exponential phase. Notably, those in batch 2 sharply decreased at 288 h, which might be a photoprotective mechanism against photodamage caused by intense photosynthesis *via* reducing chlorophyll content to slow down CO$_2$ fixation (Humby et al., 2009). In case of nitrogen assimilation, NO$_3^-$ concentration in the medium was always kept above 775 mg L^{-1} with a NO$_3^-$ uptake rate of 168.75 mg L^{-1} d^{-1} (batch 1) and 128.78 mg L^{-1} d^{-1} (batch 2), which were higher than those of the batch culture (**Table 2**); thereby the higher intracellular nitrogen contents (8.2~9.2% DW) and balanced C/N ratio around 6.0 were achieved (**Figure 2B**). These results suggested that compared to 1.25 g L^{-1} NaNO$_3$ in

shake flasks, 2.5 g L^{-1} NaNO$_3$ in 5-L photo-fermenter eliminated the N-limitation, leading to a balanced intracellular C/N ratio. Taken together, repeated fed-batch culture under higher nitrate would be a favorable option for scale-up application in CO$_2$ fixation, and the renewal rate of the medium should be optimized for further improvement.

3.3 Nutrient Composition of Biomass in a Shake Flask and 5-L Photo-Fermenter

Protein, carbohydrate, lipid, and pigments are the main nutritional components in biomass. As shown in **Figure 3A**, protein content increased to 50.1% DW in the batch culture 60.93% (batch 1) and 58.48% DW (batch 2) in repeated fed-batch culture under 2.5 g L^{-1} NaNO$_3$, which was 45.18%, 76.56%, and 69.46% higher than that of 34.51% DW under 1.25 g L^{-1} NaNO$_3$ under the optimal carbon source in shake flasks. The pigment

TABLE 3 | Amino acid and fatty acid profiles in the finally harvested biomass of autotrophic *C. subellipsoidea* under various nitrate concentrations.
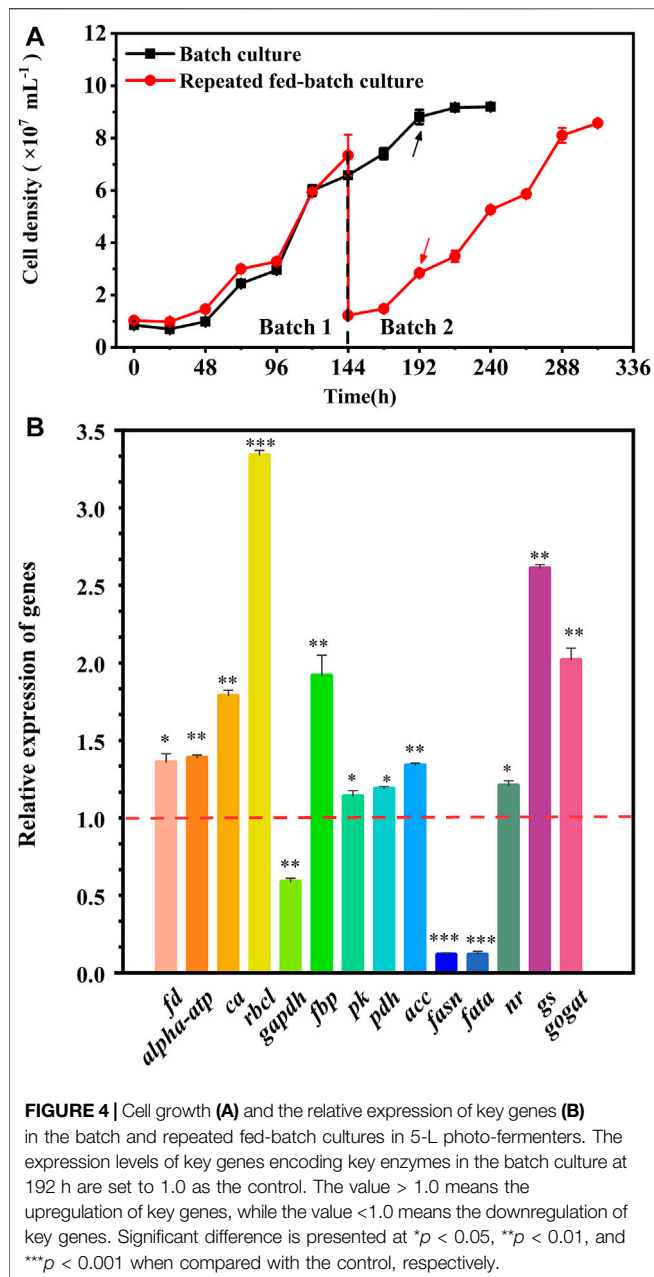
Variable	1.25 g L^{-1} NaNO$_3$ (in shake flasks)	2.5 g L^{-1} NaNO$_3$ (in 5-L photo-fermenters)		
	Batch culture	Batch culture	Repeated fed-batch culture	
			Batch 1	Batch 2
EAAs (% DW)				
Lys	1.95 ± 0.26	3.00 ± 0.11	3.44 ± 0.43	2.77 ± 0.58
Trp	0.03 ± 0.00	0.04 ± 0.01	0.04 ± 0.01	0.04 ± 0.00
Phe	1.55 ± 0.21	2.39 ± 0.09	2.80 ± 0.44	2.36 ± 0.21
Met	0.39 ± 0.08	0.76 ± 0.10	0.86 ± 0.04	0.77 ± 0.10
Thr	1.39 ± 0.23	2.22 ± 0.16	2.57 ± 0.71	2.43 ± 0.80
Ile	1.02 ± 0.02	1.83 ± 0.02	2.11 ± 0.12	1.70 ± 0.20
Leu	2.11 ± 0.23	3.64 ± 0.28	4.26 ± 0.28	3.64 ± 0.12
Val	1.51 ± 0.33	2.51 ± 0.52	2.88 ± 0.06	2.41 ± 0.05
Total EAA	9.96	16.40	18.96	16.12
NEAAs (% DW)				
His	0.67 ± 0.04	0.92 ± 0.21	1.05 ± 0.25	1.41 ± 0.02
Asp	2.76 ± 0.12	4.53 ± 0.23	5.41 ± 0.56	4.31 ± 0.52
Ser	1.39 ± 0.22	1.96 ± 0.21	2.26 ± 0.70	1.99 ± 0.21
Glu	3.43 ± 0.12	6.34 ± 0.02	7.67 ± 0.66	7.09 ± 0.11
Gly	1.65 ± 0.17	2.61 ± 0.08	2.96 ± 0.37	2.47 ± 0.33
Ala	2.25 ± 0.99	3.87 ± 0.06	4.44 ± 0.98	3.70 ± 0.67
Cys	0.10 ± 0.07	0.18 ± 0.04	0.21 ± 0.07	0.46 ± 0.01
Tyr	0.98 ± 0.06	1.77 ± 0.02	2.06 ± 0.23	2.09 ± 0.17
Arg	1.94 ± 0.22	6.10 ± 0.34	6.53 ± 0.15	6.09 ± 0.42
Pro	1.05 ± 0.01	1.91 ± 0.12	2.07 ± 0.12	2.51 ± 0.21
Total NEAAs	16.14	30.12	34.68	32.11
Fatty acids (% TFAs)				
C16:0	21.89 ± 0.13	22.31 ± 0.60	24.99 ± 0.91	26.34 ± 0.56
C18:1 (Δ9)	22.90 ± 0.43	3.59 ± 0.57	ND	ND
C18:2 (Δ9, 12)	26.71 ± 0.23	23.74 ± 0.16	25.83 ± 1.21	24.23 ± 0.52
C18:3 (Δ9, 12, 15)	22.95 ± 0.28	33.73 ± 2.17	35.60 ± 1.73	32.78 ± 0.73
C20:2 (Δ11, 14)	ND	1.94 ± 0.07	2.86 ± 0.45	2.49 ± 0.35
C20:3 (Δ11, 14, 17)	5.55 ± 0.05	10.68 ± 0.43	10.71 ± 0.19	9.22 ± 0.31
DLU	1.64	2.23	1.96	1.78
ω-6/ω-3	1.16	0.70	0.73	0.74

EAAs, essential amino acids for humans; NEAAs, non-essential amino acids; DLU, degree of lipid unsaturation; ND, not detected.

content (1.45% DW) of the batch culture in the 5-L photo-fermenter showed a 150% increase compared to that of 0.58% DW in shake flasks; while, 2.43% DW (batch 1) and 1.96% DW (batch 2) of repeated fed-batch culture in 5-L photo-fermenter were also achieved, 4.19-fold and 3.43-fold higher than that in shake flasks, respectively ($p < 0.05$). Contrarily, the culture in shake flasks resulted in higher contents of carbohydrate (31.81% DW) and lipid (31.17% DW), 1.1-~1.3-fold and 2.0-~3.0-fold higher than those (10.77~16.06% DW, 23.89~29.75% DW) in photo-fermenters ($p < 0.05$). The nitrogen level is known to alter the carbon flux, and the high level of nitrogen could accelerate protein and chlorophyll synthesis, but the limited nitrogen induced lipid synthesis (Zhu et al., 2022). It was observed that the nitrate was completely depleted on the 10th day with low intracellular nitrogen content (5.34% DW) and higher intracellular C/N ratio (10.66) in shake flasks compared to that in 5-L photo-fermenters (**Figure 1D** and **Table 1**). The low content of protein and pigments in shake flasks indicated that these nitrogenous compounds might be degraded to maintain normal metabolism under N limitation (Wu and Miao, 2014). Contrarily, in 5-L photo-fermenters, the intracellular nitrogen content (8%~9% DW) and C/N ratio (6.0) were maintained at a

suitable level, enhancing carbon allocation to protein and pigment synthesis. Attractively, the high-protein content (>60% DW) was achieved in repeated fed-batch culture (**Figure 3A**), significantly higher than that of 57.36% DW for *Chlorella* sp. (UKM2), 48.6% DW for *Scenedesmus* sp. (UKM9) (Hariz et al., 2019), and 52.3% DW for *Chlorella fusca* (Duarte et al., 2016) under autotrophic cultivation for CO$_2$ fixation. It is suggested that the high-protein biomass of *C. subellipsoidea* can be expanded to the application of algae-based protein for meat analogous and animal feed (Fu et al., 2021).

Amino acids (AAs) are the critical compounds of cell nutrition. In **Figure 3B**, the changing trend of AA content under different culture conditions was coincident with that of protein. The highest content of AAs in 5-L photo-fermenters was 53.65% DW, 2.1-fold higher than that in shake flasks. The notable difference in AA contents might also be due to the distinct nitrate level described earlier. As for the profile of AAs shown in **Table 3**, the biomass contained 18 types of AAs, including eight types of essential amino acids (EAAs) for humans. Especially, the high contents of EAAs (16.12%–18.96% DW) were found in biomass from repeated fed-batch culture, leading to attractive application

FIGURE 4 | Cell growth **(A)** and the relative expression of key genes **(B)** in the batch and repeated fed-batch cultures in 5-L photo-fermenters. The expression levels of key genes encoding key enzymes in the batch culture at 192 h are set to 1.0 as the control. The value > 1.0 means the upregulation of key genes, while the value <1.0 means the downregulation of key genes. Significant difference is presented at *$p < 0.05$, **$p < 0.01$, and ***$p < 0.001$ when compared with the control, respectively.

in healthy foods. Additionally, the typical protein diets in animal feed production require supplementation with EAAs, such as lysine (Lys), methionine (Met), threonine (Thr), and tryptophan (Trp) (Sun et al., 2020). The highest contents of these limiting EAAs reached 3.44, 0.86, 2.57, and 0.04% DW in batch 1 of repeated fed-batch culture, respectively, similar to that of soybean and corn (Lum et al., 2013). Consequently, the biomass produced by repeated fed-batch culture could be a good feedstock for animal feed production in the future (Sun et al., 2020).

Fatty acid content and percentage in total lipids are shown in **Figure 3B**, and the profile is shown in **Table 3**. Total fatty acid (TFA) contents were around 3~4% DW and 12.0 ~15.0% of total

lipids in 5-L photo-fermenters, significantly lower than that of 7.13% DW and 22.88% of total lipids in shake flasks ($p < 0.05$). The decline of TFA content could also be ascribed that a high concentration of nitrate favored for protein and chlorophylls but not for fatty acids (Gao et al., 2018). In **Table 3**, the profile of fatty acids consisted of both C16 to C18 with over 85% of TFAs, which satisfied the biodiesel quality (Wu and Miao, 2014) in all cultures. The polyunsaturated fatty acids (PUFAs) accounted for 75% of TFAs in batch 1 of repeated fed-batch culture, 1.4-fold higher than that in shake flasks. The monounsaturated fatty acids of C18:1 sharply decreased from over 22.0% to 4.0% of TFAs or less and were transformed into the PUFAs (C18:3 and C20:3) under increased nitrate in 5-L photo-fermenter. It was the opposite that the production of PUFAs (C18:2 and C18:3) in *C. vulgaris* shifted to the saturated or monounsaturated fatty acids (C18:0 and C18:1) production under N limitation (Griffiths et al., 2014). This suggested that sufficient nitrogen contributed to the synthesis of PUFAs, leading to a higher degree of lipid unsaturation (DLU) compared to the limited nitrogen (**Table 3**). Additionally, the ω-6/ω-3 ratio, being essential for human health at the ideal ratio of 1:1 (Jo et al., 2021), was from 0.70 to 1.16 in all cultures (**Table 3**), which all got close to this ideal ratio. In this case, the composition of fatty acids in the biomass of *C. subellipsoidea* satisfied with nutrient intake for human health.

In terms of composition of pigments (**Figure 3C**), high chlorophyll (Chl) content (12.9~17.9 mg g⁻¹) and a significant increase of carotenoid (Car) content (1.4~1.9 mg g⁻¹) were observed in the 5-L photo-fermenter; otherwise, only 5.11 and 0.77 mg g⁻¹ for Chl and Car contents with an obvious decline in the Chl/Car ratio from 8.0~10.3 to 6.6 in shake flasks, suggesting a relative increase of Car content under the stress of depleted nitrogen (Simionato et al., 2013). It implied that maintaining a high level of nitrate in the medium was essential for pigment synthesis. Taken together, the high-protein biomass of *C. subellipsoidea* in the present work has great potential application as feedstock for high-quality food ingredients, healthy foods, and animal feed production in the future.

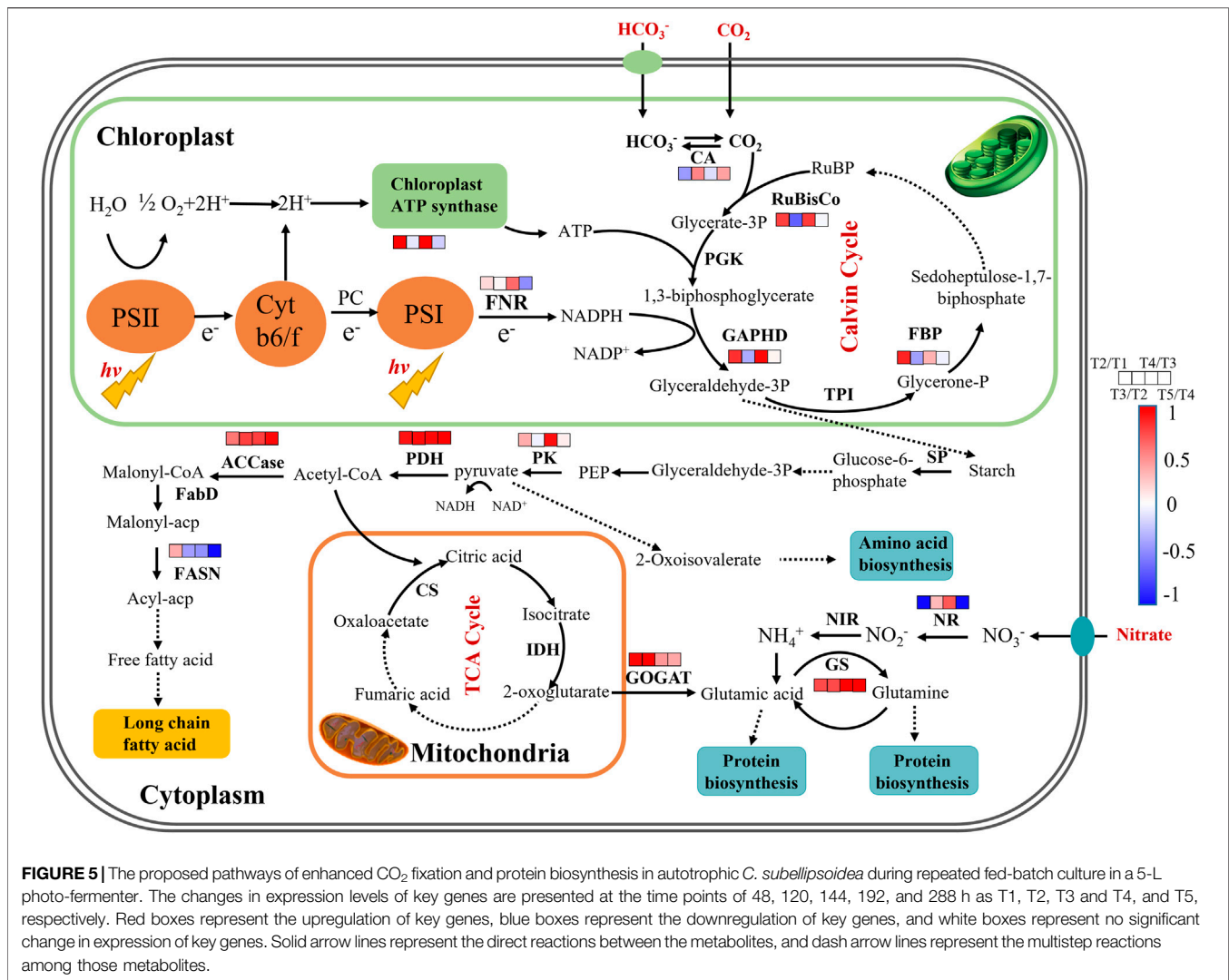## 3.4 Key Gene Expression Analysis in the Batch and Repeated Fed-Batch Cultures in 5-L Photo-Fermenters

The cell growth in the batch culture reached the stationary phase at 192 h, but a rapid growth was observed in batch 2 of repeated fed-batch culture due to the weakened light-shading (**Figure 4A**). Hence, to explore the regulation of cells' response to the variation, the fresh cells at 192 h in the batch culture and batch 2 of repeated fed-batch cultures were collected to analyze key genes' expression. As shown in **Figure 4B**, compared to that in the batch culture, the expression of ferredoxin (*fd*) and chloroplast ATP synthase (*alpha-atp*) in batch 2 was 1.36-fold and 1.39-fold upregulated, which might produce more ATP and NADPH to promote CO₂ fixation (Naduthodi et al., 2021). The expression of *rbcl* coding ribulose-1,5-bisphosphatecarboxylase/oxygenase (RuBisCo),

the critical enzyme catalyzing CO_2 fixing, was 3.34-fold upregulated, which might convert more CO_2 into glycerate-3P for cell growth (Peng et al., 2016; Li et al., 2021). It was reported that overexpression of *rbcl* in oleaginous microalga dramatically accelerated CO_2 fixation, leading to a 46% increase in biomass yield (Wei et al., 2017). The transcription of *ca* encoding carbonic anhydrase (CA) was upregulated by 1.79-fold, which perhaps provided more CO_2 for RuBisCo (Wang et al., 2015). The expression of fructose bisphosphatealdolase (*FBP*) in chloroplast was 1.92-fold upregulated, which might enhance the conversion of glyceraldehyde-3-phosphate (G3P) into fructose-1,6-biphosphate; and the overexpression of *fbp* was previously reported to enhance photosynthesis and growth rate in *Synechococcus* sp. PCC 7002 (De Porcellinis et al., 2018). But the transcription of gene coding glyceraldehyde-3-phosphate dehydrogenase (GAPDH), the key enzyme for G3P synthesis, was 0.59-fold downregulated, which did not match up with the enhanced CO_2 fixation in batch 2. The genes' expression changed rapidly, and the inconsistent transcription of *gapdh* at 192 h of repeated fed-batch culture might be affected by changing environment in the medium. Overall, the upregulated gene expression in photosynthesis assuredly enhanced CO_2 fixation in batch 2. The enhanced CO_2 fixation could provide more G3P for glycolysis, where the gene encoding pyruvate kinase (PK) was upregulated, leading to produce more ATP and pyruvate; and the gene encoding pyruvate dehydrogenase complex (PDH) was dramatically 1.19-fold upregulated; the upregulation of *pk* and *pdh* rapidly converted pyruvate into acetyl-CoA, which widely participates in TCA cycle, amino acids synthesis, and lipid metabolism (Li et al., 2021). Ordinarily, when the carbon source is no longer the limiting factor, a high level of nitrogen has a positive effect on cell growth and protein synthesis (Pancha et al., 2014). In this work, the final level of nitrate in batch 2 was 1.4-fold higher than that in the batch culture (**Table 2**); the replete nitrate might induce upregulation of genes involved in nitrogen assimilation. Consequently, the gene encoding nitrate reductase (NR) was notably upregulated to assimilate extracellular nitrogen into ammonium in cells. The gene encoding glutamine synthetase (GS), assimilating ammonium into carbon compounds in a nitrogen-rich environment, was also notably upregulated. Upregulation of the GS/GOGAT pathway promoted the integration of the carbon skeleton from the TCA cycle and assimilated nitrogen for protein synthesis. The upregulation of gene coding acetyl-CoA carboxylase (ACC) in lipid synthesis was observed, which provided an abundant substrate of malonyl-CoA for fatty acid synthesis; but the genes encoding fatty acid synthase (FASN) and fatty acyl-ACP thioesterase A (FATA), key enzymes involving in the acyl chain elongation for long-chain fatty acids, were both significantly downregulated by 0.12-fold in batch 2, which prevented the synthesis of fatty acids. Therefore, the upregulated expression of genes involved in photosynthesis and glycolysis as well as genes belonging to nitrogen assimilation could well explain the enhanced CO_2

fixation and protein synthesis in repeated fed-batch culture compared to the batch culture at the molecular level.

3.5 Proposed Regulation for the Carbon and Nitrogen Metabolic Pathway in Repeated Fed-Batch Culture

To reveal the time-dependent regulation of key genes' expression involved in carbon and nitrogen metabolism, the fresh cells were collected at 48 h (T1), 120 h (T2), and 144 h (T3) in batch 1, and 192 h (T4) and 288 h (T5) in batch 2 of repeated fed-batch culture in 5-L photo-fermenter for qRT-PCR analysis, and the expression level of the key genes was shown in **Supplementary Table S3**. As shown in **Figure 5**, most of the key genes in phosphorylation and Calvin cycle were upregulated from T1 to T2 and downregulated or kept stable from T2 to T3 at batch 1; next, they were significantly upregulated again at T4 during the exponential phase in batch 2 and then returned to the initial level or even lower at T5. The upregulated key genes from T3 to T4 related to photophosphorylation, such as *fd* and *alpha-atp*, indicated the enhanced electron transportation due to more available photons harvested by chlorophylls embedded in the thylakoid membrane at batch 2 with weakened light-shading. Meanwhile, the genes encoding RuBisCo, GAPDH, and FBP related to the Calvin cycle were significantly upregulated and then maintained stable, leading to an increased CO_2 fixation rate continuously from T2 to T5 (**Figure 2B**). Inversely, the gene coding CA showed different expression patterns with upregulation at T3 and T5 but downregulation at T2 and T4. This might be attributed to the increased pH value resulted from NO_3^- and HCO_3^- consumption in the medium, leading to more HCO_3^- and CO_3^{2-} but less CO_2; thus, the upregulation of *ca* expression could converse HCO_3^- to CO_2 for the use of RuBisco (Wang et al., 2015). Calvin cycle transformed CO_2 into C_3 compounds for glycolysis, consequently, the expression of *pk* might be closely linked with the Calvin cycle; and a similar change trend of *pk* expression was certainly observed. The enhanced glycolysis generated more pyruvate and ATP, and then a dramatical upregulation of *pdh* at all time points might immediately promote more pyruvate converted into acetyl-CoA for the TCA cycle, amino acids, and lipid metabolism (Seo et al., 2020; He et al., 2019). At the physiological and biochemical level, the content of protein was significantly higher than that of lipid under high nitrate in repeated fed-batch culture (**Figure 3A**), indicating the carbon allocation mainly to protein synthesis instead of lipid accumulation. At the transcriptional level, genes encoding GS and GOGAT were both upregulated from T2 to T5, which explained the enhanced protein synthesis; but the expression of gene encoding NR, the rate-limiting enzyme in nitrogen assimilation, did not maintain an upregulated trend. It was dramatically downregulated at T2 and T5 and only showed an upregulation at T4. In fact, the transcription change of *nr* was exactly coincident with that of nitrate consumption. The massive nitrate consumption, 552.25 mg L^{-1} (batch 1) and

FIGURE 5 | The proposed pathways of enhanced CO_2 fixation and protein biosynthesis in autotrophic *C. subellipsoidea* during repeated fed-batch culture in a 5-L photo-fermenter. The changes in expression levels of key genes are presented at the time points of 48, 120, 144, 192, and 288 h as T1, T2, T3 and T4, and T5, respectively. Red boxes represent the upregulation of key genes, blue boxes represent the downregulation of key genes, and white boxes represent no significant change in expression of key genes. Solid arrow lines represent the direct reactions between the metabolites, and dash arrow lines represent the multistep reactions among those metabolites.

646.65 mg L^{-1} (batch 2), accounting for over 30% of total nitrate in the medium, was observed on the first two days in each batch culture, while the slow uptake of nitrate in the later period (**Figure 2B**). It was reported that the algal cells could take in nitrogen exceeded immediate demand under sufficient nitrogen, allowing organisms to build an "intracellular nitrogen pool" for use in times of scarcity. The nitrogen regulation strategy is called "luxury consumption" in nitrogen assimilation of algae (Bugbee, 2014). The sufficient nitrate transported into the cell induced the high expression level of *nr*, reducing nitrate to nitrite at T1 and T4; and the downregulated expression of *nr* corresponded to slow uptake of nitrate at T2, T3, and T5. In terms of lipid synthesis, the expression of gene coding FASN (rate-limiting enzyme) was sharply downregulated from T3 to T5, resulting in the restriction of fatty acid biosynthesis, even though the expression of *acc* was significantly upregulated. In summary, through analyzing the expression of key genes involved in central carbon and nitrogen metabolism, the underlying molecular mechanisms for regulation of CO_2 fixation and allocation of carbon flow were primarily elaborated. These achievements would be meaningful for an in-depth understanding of other microalgal responses to different cultivation modes under relative high-level nitrogen.

4 CONCLUSION

In this study, a promising approach of hybrid chemical absorption–biofixation of CO_2 was developed to enhance CO_2 fixation and biomass production. Repeated fed-batch culture in a 5-L photo-fermenter resulted in high-protein biomass production, and then, the analysis of key gene expression involved in carbon and nitrogen metabolism revealed the regulation of carbon allocation under high-efficient CO_2 fixation. The present results proved that *C. subellipsoide* is a promising cell factory for high-efficient CO_2 fixation with high-protein biomass coproduction, thus expanding the application of this oleaginous microalga in carbon emission reduction and protein production instead of oil production for green manufacturing.

DATA AVAILABILITY STATEMENT

The original contributions presented in the study are included in the article/**Supplementary Material**; further inquiries can be directed to the corresponding author.

AUTHOR CONTRIBUTIONS

YL: data collection and curation, data analysis, conceptualization, and draft writing and editing. DW: conceptualization, supervision, reviewing, editing, and funding acquisition. WC: reviewing, suggestion, and editing.

REFERENCES

Adams, C., and Bugbee, B. (2014). Nitrogen Retention and Partitioning at the Initiation of Lipid Accumulation in Nitrogen-Deficient Algae. *J. Phycol.* 50, 356–365. doi:10.1111/jpy.12167

Blanc, G., Agarkova, I., Grimwood, J., Kuo, A., Brueggeman, A., Dunigan, D. D., et al. (2012). The Genome of the Polar Eukaryotic Microalga Coccomyxa Subellipsoidea Reveals Traits of Cold Adaptation. *Genome Biol.* 13, R39. doi:10.1186/gb-2012-13-5-r39

Blunden, J., and Arndt, D. S. (2020). State of the Climate in 2019. *Bull. Am. Meteorol. Soc.* 101, S1–S429. doi:10.1175/2020BAMSStateoftheClimate.1

Chen, J.-H., Wei, D., Lim, P.-E., Xie, J., and Chen, W. N. (2021). Screening and Effect Evaluation of Chemical Inducers for Enhancing Astaxanthin and Lipid Production in Mixotrophic Chromochloris Zofingiensis. *J. Appl. Phycol.* 34, 159–176. doi:10.1007/s10811-021-02618-6

Chen, J., Liu, X., Wei, D., and Chen, G. (2015). High Yields of Fatty Acid and Neutral Lipid Production from Cassava Bagasse Hydrolysate (CBH) by Heterotrophic Chlorella Protothecoides. *Bioresour. Technol.* 191, 281–290. doi:10.1016/j.biortech.2015.04.116

Chen, W., Tong, H., and Liu, H. (2012). Effects of Nitrate on Nitrite Toxicity to Microcystis Aeruginosa. *Mar. Pollut. Bull.* 64, 1106–1111. doi:10.1016/j.marpolbul.2012.04.006

Chen, Y., and Vaidyanathan, S. (2013). Simultaneous Assay of Pigments, Carbohydrates, Proteins and Lipids in Microalgae. *Anal. Chim. Acta* 776, 31–40. doi:10.1016/j.aca.2013.03.005

Cheng, D., Li, X., Yuan, Y., Yang, C., Tang, T., Zhao, Q., et al. (2019). Adaptive Evolution and Carbon Dioxide Fixation of Chlorella Sp. In Simulated Flue Gas. *Sci. Total Environ.* 650, 2931–2938. doi:10.1016/j.scitotenv.2018.10.070

Corteggiani Carpinelli, E., Telatin, A., Vitulo, N., Forcato, C., D'Angelo, M., Schiavon, R., et al. (2014). Chromosome Scale Genome Assembly and Transcriptome Profiling of Nannochloropsis Gaditana in Nitrogen Depletion. *Mol. Plant* 7, 323–335. doi:10.1093/mp/sst120

De Porcellinis, A. J., Nørgaard, H., Brey, L. M. F., Erstad, S. M., Jones, P. R., Heazlewood, J. L., et al. (2018). Overexpression of Bifunctional Fructose-1,6-Bisphosphatase/Sedoheptulose-1,7-Bisphosphatase Leads to Enhanced Photosynthesis and Global Reprogramming of Carbon Metabolism in Synechococcus Sp. PCC 7002. *Metab. Eng.* 47, 170–183. doi:10.1016/j.ymben.2018.03.001

Dean, A. P., Sigee, D. C., Estrada, B., and Pittman, J. K. (2010). Using FTIR Spectroscopy for Rapid Determination of Lipid Accumulation in Response to Nitrogen Limitation in Freshwater Microalgae. *Bioresour. Technol.* 101, 4499–4507. doi:10.1016/j.biortech.2010.01.065

Duarte, J. H., Fanka, L. S., and Costa, J. A. V. (2016). Utilization of Simulated Flue Gas Containing CO2, SO2, NO and Ash for Chlorella Fusca Cultivation. *Bioresour. Technol.* 214, 159–165. doi:10.1016/j.biortech.2016.04.078

Fu, Y., Chen, T., Chen, S. H. Y., Liu, B., Sun, P., Sun, H., et al. (2021). The Potentials and Challenges of Using Microalgae as an Ingredient to Produce Meat Analogues. *Trends Food Sci. Technol.* 112, 188–200. doi:10.1016/j.tifs.2021.03.050

Gao, B., Liu, J., Zhang, C., and Van De Waal, D. B. (2018). Biological Stoichiometry of Oleaginous Microalgal Lipid Synthesis: The Role of N:P Supply Ratios and Growth Rate on Microalgal Elemental and Biochemical Composition. *Algal Res.* 32, 353–361. doi:10.1016/j.algal.2018.04.019

Gardner, R. D., Cooksey, K. E., Mus, F., Macur, R., Moll, K., Eustance, E., et al. (2012). Use of Sodium Bicarbonate to Stimulate Triacylglycerol Accumulation in the Chlorophyte Scenedesmus Sp. And the Diatom Phaeodactylum Tricornutum. *J. Appl. Phycol.* 24, 1311–1320. doi:10.1007/s10811-011-9782-0

Griffiths, M. J., Van Hille, R. P., and Harrison, S. T. L. (2014). The Effect of Nitrogen Limitation on Lipid Productivity and Cell Composition in Chlorella Vulgaris. *Appl. Microbiol. Biotechnol.* 98, 2345–2356. doi:10.1007/s00253-013-5442-4

Hariz, H. B., Takriff, M. S., Mohd Yasin, N. H., Ba-Abbad, M. M., and Mohd Hakimi, N. I. N. (2019). Potential of the Microalgae-Based Integrated Wastewater Treatment and CO2 Fixation System to Treat Palm Oil Mill Effluent (POME) by Indigenous Microalgae; Scenedesmus Sp. And Chlorella Sp. *J. Water Process Eng.* 32, 100907. doi:10.1016/j.jwpe.2019.100907

He, L., Jing, Y., Shen, J., Li, X., Liu, H., Geng, Z., et al. (2019). Mitochondrial Pyruvate Carriers Prevent Cadmium Toxicity by Sustaining the TCA Cycle and Glutathione Synthesis. *Plant Physiol.* 180, 198–211. doi:10.1104/pp.18.01610

Huang, Y., Li, P., Chen, G., Peng, L., and Chen, X. (2018). The Production of Cyanophycin Carbon under Nitrogen-Limited Cultivation and its Potential for Nitrate Removal. *Chemosphere* 190, 1–8. doi:10.1016/j.chemosphere.2017.09.125

Humby, P. L., Cunningham, M. L., Saunders, H. L., Price, J. A., and Durnford, D. G. (2009). Compartmental Cross-Talk in the Regulation of Light Harvesting Complex Transcription under Short-Term Light and Temperature Stress in Chlamydomonas Reinhardtii. *Botany* 87, 375–386. doi:10.1139/b09-005

Jo, H., Kim, M., Cho, H., Ha, B.-K., Kang, S., Song, J. T., et al. (2021). Identification of a Potential Gene for Elevating ω-3 Concentration and its Efficiency for Improving the ω-6/ω-3 Ratio in Soybean. *J. Agric. Food Chem.* 69, 3836–3847. doi:10.1021/acs.jafc.0c05830

Li, J., Pan, K., Tang, X., Li, Y., Zhu, B., and Zhao, Y. (2021). The Molecular Mechanisms of Chlorella Sp. Responding to High CO2: A Study Based on Comparative Transcriptome Analysis between Strains with High- and low-CO2 Tolerance. *Sci. Total Environ.* 763, 144185. doi:10.1016/j.scitotenv.2020.144185

Lohman, E. J., Gardner, R. D., Pedersen, T., Peyton, B. M., Cooksey, K. E., and Gerlach, R. (2015). Optimized Inorganic Carbon Regime for Enhanced Growth and Lipid Accumulation in Chlorella Vulgaris. *Biotechnol. Biofuels* 8, 82. doi:10.1186/s13068-015-0265-4

Lum, K. K., Kim, J., and Lei, X. G. (2013). Dual Potential of Microalgae as a Sustainable Biofuel Feedstock and Animal Feed. *J. Anim. Sci. Biotechnol.* 4, 53. doi:10.1186/2049-1891-4-53

Miller, R., Wu, G., Deshpande, R. R., Vieler, A., Gärtner, K., Li, X., et al. (2010). Changes in Transcript Abundance in Chlamydomonas Reinhardtii Following Nitrogen Deprivation Predict Diversion of Metabolism. *Plant Physiol.* 154, 1737–1752. doi:10.1104/pp.110.165159

Moejes, F. W., Matuszyńska, A., Adhikari, K., Bassi, R., Cariti, F., Cogne, G., et al. (2017). A Systems-wide Understanding of Photosynthetic Acclimation in Algae and Higher Plants. *J. Exp. Bot.* 68, 2667–2681. doi:10.1093/jxb/erx137

FUNDING

SUPPLEMENTARY MATERIAL

The Supplementary Material for this article can be found online at: https://www.frontiersin.org/articles/10.3389/fbioe.2022.921024/full#supplementary-material

Naduthodi, M. I. S., Claassens, N. J., D'Adamo, S., Van Der Oost, J., and Barbosa, M. J. (2021). Synthetic Biology Approaches to Enhance Microalgal Productivity. *Trends Biotechnol.* 39, 1019–1036. doi:10.1016/j.tibtech.2020.12.010

Pancha, I., Chokshi, K., George, B., Ghosh, T., Paliwal, C., Maurya, R., et al. (2014). Nitrogen Stress Triggered Biochemical and Morphological Changes in the Microalgae Scenedesmus Sp. CCNM 1077. *Bioresour. Technol.* 156, 146–154. doi:10.1016/j.biortech.2014.01.025

Peng, H., Wei, D., Chen, G., and Chen, F. (2016). Transcriptome Analysis Reveals Global Regulation in Response to CO_2 Supplementation in Oleaginous Microalga Coccomyxa Subellipsoidea C-169. *Biotechnol. Biofuels* 9, 151. doi:10.1186/s13068-016-0571-5

Pielke, R., Burgess, M. G., and Ritchie, J. (2022). Plausible 2005-2050 Emissions Scenarios Project between 2 °C and 3 °C of Warming by 2100. *Environ. Res. Lett.* 17, 024027. doi:10.1088/1748-9326/ac4ebf

Pilon, L., Berberoğlu, H., and Kandilian, R. (2011). Radiation Transfer in Photobiological Carbon Dioxide Fixation and Fuel Production by Microalgae. *J. Quantitative Spectrosc. Radiat. Transf.* 112, 2639–2660. doi:10.1016/j.jqsrt.2011.07.004

Rodas-Zuluaga, L. I., Castañeda-Hernández, L., Castillo-Vacas, E. I., Gradiz-Menjivar, A., López-Pacheco, I. Y., Castillo-Zacarías, C., et al. (2021). Bio-capture and Influence of CO_2 on the Growth Rate and Biomass Composition of the Microalgae Botryococcus Braunii and Scenedesmus Sp. *J. CO2 Util.* 43, 101371. doi:10.1016/j.jcou.2020.101371

Ruiz, J., Olivieri, G., De Vree, J., Bosma, R., Willems, P., Reith, J. H., et al. (2016). Towards Industrial Products from Microalgae. *Energy Environ. Sci.* 9, 3036–3043. doi:10.1039/c6ee01493c

Seo, S., Kim, J., Lee, J.-W., Nam, O., Chang, K. S., and Jin, E. (2020). Enhanced Pyruvate Metabolism in Plastids by Overexpression of Putative Plastidial Pyruvate Transporter in Phaeodactylum Tricornutum. *Biotechnol. Biofuels* 13, 120. doi:10.1186/s13068-020-01760-6

Simionato, D., Block, M. A., La Rocca, N., Jouhet, J., Maréchal, E., Finazzi, G., et al. (2013). The Response of Nannochloropsis Gaditana to Nitrogen Starvation Includes De Novo Biosynthesis of Triacylglycerols, a Decrease of Chloroplast Galactolipids, and Reorganization of the Photosynthetic Apparatus. *Eukaryot. Cell* 12, 665–676. doi:10.1128/EC.00363-12

Song, C., Liu, J., Xie, M., Qiu, Y., Chen, G., Qi, Y., et al. (2019a). Intensification of a Novel Absorption-Microalgae Hybrid CO_2 Utilization Process via Fed-Batch Mode Optimization. *Int. J. Greenh. Gas Control* 82, 1–7. doi:10.1016/j.ijggc.2019.01.001

Song, C., Liu, Q., Qi, Y., Chen, G., Song, Y., Kansha, Y., et al. (2019b). Absorption-Microalgae Hybrid CO_2 Capture and Biotransformation Strategy-A Review. *Int. J. Greenh. Gas Control* 88, 109–117. doi:10.1016/j.ijggc.2019.06.002

Song, C., Qiu, Y., Li, S., Liu, Z., Chen, G., Sun, L., et al. (2019c). A Novel Concept of Bicarbonate-Carbon Utilization via an Absorption-Microalgae Hybrid Process Assisted with Nutrient Recycling from Soybean Wastewater. *J. Clean. Prod.* 237, 117864. doi:10.1016/j.jclepro.2019.117864

Su, Y. (2021). Revisiting Carbon, Nitrogen, and Phosphorus Metabolisms in Microalgae for Wastewater Treatment. *Sci. Total Environment* 762, 144590. doi:10.1016/j.scitotenv.2020.144590

Sun, Y., Liao, Q., Huang, Y., Xia, A., Fu, Q., Zhu, X., et al. (2016). Integrating Planar Waveguides Doped with Light Scattering Nanoparticles into a Flat-Plate Photobioreactor to Improve Light Distribution and Microalgae Growth. *Bioresour. Technol.* 220, 215–224. doi:10.1016/j.biortech.2016.08.063

Sun, Y., Teng, T., Bai, G., Qiu, S., Shi, B., Ju, D., et al. (2020). Protein-Restricted Diet Balanced for Lysine, Methionine, Threonine, and Tryptophan for Nursery Pigs Elicits Subsequent Compensatory Growth and Has Long Term Effects on Protein Metabolism and Organ Development. *Animal Feed Sci. Technol.* 270, 114712. doi:10.1016/j.anifeedsci.2020.114712

Tu, Z., Liu, L., Lin, W., Xie, Z., and Luo, J. (2018). Potential of Using Sodium Bicarbonate as External Carbon Source to Cultivate Microalga in Non-Sterile Condition. *Bioresour. Technol.* 266, 109–115. doi:10.1016/j.biortech.2018.06.076

Wang, C., Wang, Z., Luo, F., and Li, Y. (2017). The Augmented Lipid Productivity in an Emerging Oleaginous Model Alga Coccomyxa Subellipsoidea by Nitrogen Manipulation Strategy. *World J. Microbiol. Biotechnol.* 33, 160. doi:10.1007/s11274-017-2324-4

Wang, Q., Yu, Z., and Wei, D. (2020). High-yield Production of Biomass, Protein and Pigments by Mixotrophic Chlorella Pyrenoidosa through the Bioconversion of High Ammonium in Wastewater. *Bioresour. Technol.* 313, 123499. doi:10.1016/j.biortech.2020.123499

Wang, Y., Stessman, D. J., and Spalding, M. H. (2015). The CO 2 Concentrating Mechanism and Photosynthetic Carbon Assimilation in Limiting CO 2 : How Chlamydomonas Works against the Gradient. *Plant J.* 82, 429–448. doi:10.1111/tpj.12829

Wang, Z., Cheng, J., Song, W., Du, X., and Yang, W. (2022). CO_2 Gradient Domestication Produces Gene Mutation Centered on Cellular Light Response for Efficient Growth of Microalgae in 15% CO_2 from Flue Gas. *Chem. Eng. J.* 429, 131968. doi:10.1016/j.cej.2021.131968

Wang, Z., Luo, F., Wang, Z., Zhou, R., Tang, Y., and Li, Y. (2019). The Potential Growth and Lipid Accumulation in Coccomyxa Subellipsoidea Triggered by Glucose Combining with Sodium Acetate. *World J. Microbiol. Biotechnol.* 35, 110. doi:10.1007/s11274-019-2682-1

Wang, Z., Wen, X., Xu, Y., Ding, Y., Geng, Y., and Li, Y. (2018). Maximizing CO_2 Biofixation and Lipid Productivity of Oleaginous Microalga Graesiella Sp. WBG-1 via CO2-regulated pH in Indoor and Outdoor Open Reactors. *Sci. Total Environ.* 619-620, 827–833. doi:10.1016/j.scitotenv.2017.10.127

Wei, L., Wang, Q., Xin, Y., Lu, Y., and Xu, J. (2017). Enhancing Photosynthetic Biomass Productivity of Industrial Oleaginous Microalgae by Overexpression of RuBisCO Activase. *Algal Res.* 27, 366–375. doi:10.1016/j.algal.2017.07.023

Wu, H., and Miao, X. (2014). Biodiesel Quality and Biochemical Changes of Microalgae Chlorella Pyrenoidosa and Scenedesmus Obliquus in Response to Nitrate Levels. *Bioresour. Technol.* 170, 421–427. doi:10.1016/j.biortech.2014.08.017

Yadav, G., Mathimani, T., Sekar, M., Sindhu, R., and Pugazhendhi, A. (2021). Strategic Evaluation of Limiting Factors Affecting Algal Growth - An Approach to Waste Mitigation and Carbon Dioxide Sequestration. *Sci. Total Environ.* 796, 149049. doi:10.1016/j.scitotenv.2021.149049

Yadav, G., Meena, D. K., Sahoo, A. K., Das, B. K., and Sen, R. (2020). Effective Valorization of Microalgal Biomass for the Production of Nutritional Fish-Feed Supplements. *J. Clean. Prod.* 243, 118697. doi:10.1016/j.jclepro.2019.118697

Zhou, W., Wang, J., Chen, P., Ji, C., Kang, Q., Lu, B., et al. (2017). Bio-Mitigation of Carbon Dioxide Using Microalgal Systems: Advances and Perspectives. *Renew. Sustain. Energy Rev.* 76, 1163–1175. doi:10.1016/j.rser.2017.03.065

Zhu, W., Wei, D., and Pohnert, G. (2022). The Thermoacidophilic Red Alga Galdieria Sulphuraria is a Highly Efficient Cell Factory for Ammonium Recovery from ultrahigh-NH4+ Industrial Effluent with Co-production of High-Protein Biomass by Photo-Fermentation. *Chem. Eng. J.* 438, 135598. doi:10.1016/j.cej.2022.135598

Zhu, C., Zhai, X., Xi, Y., Wang, J., Kong, F., Zhao, Y., et al. (2020). Efficient CO_2 Capture from the Air for High Microalgal Biomass Production by a Bicarbonate Pool. *J. CO2 Util.* 37, 320–327. doi:10.1016/j.jcou.2019.12.023